The Journal of Neuroscience, March 1994, 14(3): 1463–1476

Functional Expression and Characterization of Human D_2 and D_3 Dopamine Receptors

Marc N. Potenza,[1,2] Gerard F. Graminski,[2,3] Claudia Schmauss,[5] and Michael R. Lerner[2,3,4]

[1]Department of Cell Biology, [2]Department of Internal Medicine, [3]Howard Hughes Medical Institute, and [4]Department of Pharmacology, Boyer Center for Molecular Medicine, Yale University School of Medicine, New Haven, Connecticut 06510 and [5]Department of Psychiatry and Brookdale Center for Molecular Biology, Mount Sinai School of Medicine, New York, New York 10029

Functional characteristics of human D_2 and D_3 receptors (DRs) were examined using a new bioassay suited for the study of G_i-protein–coupled receptors (G_iRs). The bioassay utilizes pigment granule aggregation within cultured *Xenopus laevis* melanophores for the quantitative evaluation of ligands as agonists or antagonists upon particular G_iRs. Initial feasibility studies were performed by analyzing a melanocyte receptor endogenous to the melanophores. In dose-dependent manners, melatonin inhibited melatonin-stimulating hormone–induced cAMP accumulation and caused pigment aggregation that could be monitored over time. Next, melanophores were transiently transfected with cDNAs coding for the human D_{2B}R (short form) and D_3R. Expression of either receptor conferred upon the cells the ability to aggregate their melanosomes in response to selective dopaminergic agonists. The same ligands also inhibited cAMP accumulation within the transfected melanophores, and the agonist-induced pigment aggregation was shown to be sensitive to pertussis toxin. EC_{50} and IC_{50} value determinations revealed that agonists activated the D_2R and D_3R at similar concentrations, while each of the antagonists displaying an effect was more potent upon the D_2R. The results reveal functional similarities and differences between the D_2R and D_3R.

[Key words: melanophores, G-protein–coupled receptors, dopamine receptors, cAMP, drug screening, signal transduction]

The neurotransmitter dopamine mediates many processes in the CNS, including motor control, emotional behavior, and cognitive actions. Improper or abnormal functioning of dopaminergic pathways is implicated in such pathological states as Parkinson's disease, schizophrenia, depression, and drug abuse (Snyder, 1973; Hornykiewicz, 1986; Richelson, 1988; Davis et al., 1991; Muscat et al., 1992; Caine and Koob, 1993). Dopamine is believed to exert its effects in the CNS through three major pathways: the nigrostriatal, mesolimbic, and mesocortical (Dahlstrom and Fuxe, 1964). Each route is associated with particular functions. For example, the nigrostriatal connections, which degenerate in Parkinson's disease, coordinate motor control, while the mesolimbic or mesocortical systems are believed to be involved in affective thought processes (Stevens, 1973; Robbins, 1990; Healy, 1991).

The effects of dopamine are primarily mediated by a family of G-protein–coupled receptors (GRs; Civelli et al., 1991; Sibley and Monsma, 1992). According to differences in their pharmacological profiles and the intracellular signaling pathways they employ upon activation, dopamine receptors (DRs) have classically been divided into two major groups: D_1Rs and D_2Rs (Kebabian and Greengard, 1971; Kebabian et al., 1972; Stoof and Kebabian, 1984; Seeman and Grigoriadis, 1987; Seeman and Niznik, 1988). Recent advances in molecular biology have revealed at least five human genes encoding DRs (Civelli et al., 1991; Sibley and Monsma, 1992). The pharmacological classification traditionally employed for DRs correlates well with the molecular characterization of the receptors. For example, in addition to sharing high degrees of sequence similarity, the genes encoding the D_1-like D_1R and D_5R are both intronless (Dearry et al., 1990; Sunahara et al., 1990, 1991; Zhou et al., 1990; Tiberi et al., 1991). In contrast, those coding for the D_2-like D_2R, D_3R, and D_4R contain similarly distributed introns (Dal Toso et al., 1989; Grandy et al., 1989; Chio et al., 1990; Sokoloff et al., 1990; Stormann et al., 1990; Van Tol et al., 1991). The genes encoding both the D_2R and D_3R have been demonstrated to produce alternatively spliced transcripts leading to the generation of multiple gene products (Dal Toso et al., 1989; Giros et al., 1991; Snyder et al., 1991), and that corresponding to the D_4R has been shown to contain variable numbers of a 48 base pair repeat (Van Tol et al., 1992). Interestingly, many of the alternatively spliced or variant products differ in the third intracytoplasmic loop region of the receptor, the primary region of GRs believed to determine receptor interaction with G-proteins (Kubo et al., 1988; Palm et al., 1989; Cheung et al., 1991; Lechleiter et al., 1991; Liggett et al., 1991; Munch et al., 1991).

The roles of individual D_2-like receptors, especially with respect to their links to schizophrenia, are currently a focus of research interest. Receptor localization has provided some insight. The D_2R, expressed at high levels in many areas receiving dopaminergic innervation, has been suggested as mediating the extrapyramidal symptoms experienced in patients taking classical neuroleptics, and the D_3R, expressed in a more restricted

Received Apr. 9, 1993; revised July 19, 1993; accepted Sept. 13, 1993.

We thank A. Roby-Shemkovitz and L. Golyvan for technical assistance, T. McClintock for help with video microscopy, W. Clark for useful discussions, J. Howe for informative discussions and input, M. Stocks and J. Clark for critical reading of the manuscript, and P. Broccoli for assistance in preparation of the manuscript. The work was supported by the Burroughs Wellcome Fund, G. D. Searle & Co., the Office of Naval Research, the Medical Scientist Training Program, and the Howard Hughes Medical Institute.

Correspondence should be addressed to Michael R. Lerner, Yale University School of Medicine, Boyer Center for Molecular Medicine, Room 254, 295 Congress Avenue, P.O. Box 9812, New Haven, CT 06536-0812.

fashion predominantly in phylogenetically ancient brain regions, has been postulated as impacting upon more emotive thought processes (Bouthenet et al., 1991; Guennoun and Bloch, 1991; Levesque et al., 1992). The D_4R has also been suggested as a possible site of neuroleptic action, as clozapine exhibits higher affinity for the D_4R than for either the D_3R or the D_2R (Kane et al., 1988; Van Tol et al., 1991; Seeman, 1992).

Other aspects of receptor function have been investigated in order to evaluate similarities and differences between the D_2-like receptors. Pharmacological characterization of the D_2-like receptors has revealed a large degree of similarity in terms of binding affinities and rank order potencies of agonists and antagonists, with a few notable exceptions (Sokoloff et al., 1990, 1992; Van Tol et al., 1991). As explored to date, the second messenger systems employed upon activation of the receptors reveal some similarities and some differences. The effects of DRs upon intracellular cAMP levels are among the best characterized in terms of signal transduction mechanisms. For approximately 20 years, D_1R-like receptor activation has been correlated with increases and D_2-like receptor with decreases in intracellular cAMP levels (Kebabian and Greengard, 1971; Kebabian et al., 1972; Seeman and Grigoriadis, 1987). The D_2R, the first DR to be molecularly cloned, has been demonstrated to associate robustly with G-proteins to inhibit adenylyl cyclase (AC; Dal Toso et al., 1989; Neve et al., 1989). More recently, the D_4R has also been shown to mediate inhibition of AC (Cohen et al., 1992).

Although the cDNA encoding the D_3R was isolated approximately 3 years ago, conclusive determination of the intracellular signaling pathway used upon receptor activation has proven to be unexpectedly difficult. Expression of either the rat or human forms of the D_3R in heterologous systems results in weak or negligible association with G-proteins and either minor and inconsistent or no discernable changes in the second messenger levels examined (Sokoloff et al., 1990, 1992; Coco and Kilts, 1992; Freedman et al., 1992; Tang et al., 1992). For these reasons, although binding studies of ligands upon the D_3R have been performed, the more informative data concerning ligand-induced alterations in cellular functioning have not been acquired.

In order to explore the functional characteristics of the human D_3R with respect to a human D_2R, a quantitative bioassay designed for the study of G_iRs was developed. Recently, we have described rapid, functional, microtiter-based assays for evaluating the effects of ligands upon GRs that activate AC (Potenza and Lerner, 1992; Potenza et al., 1992) or phospholipase C (PLC; Graminski et al., 1993). In these assays, cells transfected with GR-encoding plasmid DNA are seeded into microtiter plates and exposed initially to melatonin to induce pigment aggregation and then to a variety of drugs at multiple concentrations. Receptor activation inducing cAMP accumulation or diacylglycerol generation causes melanosome dispersion and changes in phototransmission that can be quantitated using a microtiter plate reader. Time course analyses, EC_{50} and IC_{50} calculations, and rank order potency determinations can be made for ligands upon specific GRs. The results of the assay are reproducible and can be determined in less than 30 min.

Here, the development of a quantitative functional bioassay utilizing pigment aggregation as the reporter for ligand-mediated activation of G_iRs is described. A melatonin receptor endogenous to the melanophores is characterized to verify the integrity of the system. Next the assay is used to compare the actions of two human dopamine receptors, $D_{2B}R$ and D_3R, in transiently transfected melanophores. Expression of each receptor allowed for dopaminergic agonist-induced aggregation that was blocked by dopaminergic antagonists, was inhibited by pretreatment with pertussis toxin (PTX) and resulted in inhibition of melanocyte-stimulating hormone (MSH)-induced cAMP accumulation. The melanophores provide the first demonstration of consistent functional activation of the D_3R, and the abilities of dopaminergic ligands to stimulate or antagonize the DRs are discussed with respect to the receptors' previously reported ligand binding profiles and G-protein interactions.

Materials and Methods

Cell culture. Xenopus laevis melanophores and fibroblasts were propagated as described previously (Potenza and Lerner, 1991).

Microtiter plate assays. Microtiter plate assays were modified from protocols described previously (Potenza and Lerner, 1992; Potenza et al., 1992; Graminski et al., 1993). Wild type (WT) or electroporated cells were seeded in 100 μl of fibroblast-conditioned medium into microtiter plates (Falcon or SLT/Tecan) such that the cells were superconfluent [10,000–30,000 (Falcon) or 9000–18,000 (SLT/Tecan) cells/well]. Two days following plating, the cells in each well were washed once with and then incubated overnight in 50 μl of Excell [70% Ex-Cell 300 A supplemented with 7% Ex-Cell B (JRH Scientific)]. Fifty microliters of Excell were added to each well, and the cells were incubated for 30 min in white light [75 W bulb (General Electric)] at 1–1.4 mW/cm^2 (light source located 12–18 inches from the cells) as measured by a J16 or J17 digital photometer (Tektronix). Fifty microliters of Excell containing three times the final concentrations of ligands were added to the wells at "time zero," and the cells were maintained in white light as above for the duration of the experiment except for the 10–12 sec periods during which measurements were being performed by the microtiter plate reader (SLT/Tecan). All ligands used were obtained from either Sigma or Research Biochemicals Inc. (RBI), with the exception of melatonin and MSH, which were generous gifts of Aaron Lerner (Yale University). 7-OH DPAT [7-hydroxy-2-(*N,N*-dipropylamino)tetralin] was provided by RBI as part of the Chemical Synthesis Program of the National Institute of Mental Health, Contract 278-90-0007 (BS). All drug preparations were made upon the day of use, except for melatonin, which was diluted from a stock solution stored in ethanol at −20°C. In the studies employing pertussis toxin (PTX; Sigma), the cells were incubated overnight (14–20 hr) in 100 μl of Excell containing the indicated concentration of PTX. Cells were exposed to white light as described above for 30 min [WT, (see Fig. 7*A,B*), D_3R-expressing (7*E,F*)] or 90 min [WT (data not shown), D_2R-expressing (Fig. 7*C,D*)] prior to the addition of ligands in 50 μl of Excell to the final indicated concentration. No significant variation in PTX sensitivity was observed in WT cells pretreated with light for 30 or 90 min, nor were there any discernable differences when varying the time of incubation with PTX from 14 to 20 hr (data not shown). Data acquisition and reduction were performed as described previously (Potenza and Lerner, 1992). When curve fitting the data, the general equation employed was $y = (y_{min} + (y_{max})(10^x))/(10^x + 1)$, where $x = \log[\text{ligand}] - \log(EC_{50}$ or $IC_{50})$, $y = \Delta(A_F/A_I - 1)$, as described in the Results, y_{min} = minimum plateau value of y, and y_{max} = maximum plateau value of y (Graminski et al., 1993).

Cyclic AMP quantitation. cAMP studies were performed essentially as described previously with the following modifications (Potenza and Lerner, 1992). Transfected or WT cells were seeded at superconfluency (approximately 200,000–300,000 cells per well) into the wells of a 24-well tissue culture dish (Falcon). Two days following plating, the cells in each well were washed once with and then incubated overnight in 1.5 ml of Excell. Fifteen microliters of Excell containing drugs at 100-fold the final concentrations were added in the dark under red light and the cells incubated for 30 min in the dark to avoid cAMP changes secondary to photostimulation (Daniolos et al., 1990). Upon conclusion of the incubation, the protocol for cAMP extraction and determination was followed as described elsewhere (Potenza and Lerner, 1992). The data displayed in any one graph were obtained from experiments performed on the same day to avoid day-to-day variations in intracellular cAMP levels.

Plasmid DNA constructs. The expression vector pcDNAI/NEO was obtained from Invitrogen. The pcDNAI/NEO construct (pcD2R) containing a cDNA copy of a D_{2B} (short form) dopamine receptor, isolated from human brain mRNA by polymerase chain reaction (PCR) and

verified by restriction enzyme analysis and sequencing, was a generous gift of Michael Graziano (Merck). The plasmid construct pJGD2R was created by ligating the 1.4 kilobase HindIII-XbaI fragment into the HindIII-XbaI–digested pJG3.6 vector such that the gene is under the transcriptional regulation of the CMV promoter (Graminski et al., 1993). The *lacZ*-containing plasmid pON260 was a generous gift of Susan Amara (Vollum Institute), and the *lacZ*-containing plasmid pJG3.6lacz was constructed as described elsewhere (Graminski et al., 1993). The plasmid construct containing a copy of the gene encoding a human D_3R was constructed by amplifying the cDNA coding for the receptor by PCR and introducing it under the transcriptional regulation of the CMV promoter into the expression vector pRC/CMV (Invitrogen). Plasmid DNA constructions and amplification were done by standard protocols. All restriction enzymes were purchased from Boehringer-Mannheim.

Transfections. Plasmid DNA was transfected into the melanophores by the method of electroporation (Potter et al., 1984; Potter, 1988) using a Gene Pulser apparatus (Bio-Rad) at a capacitance setting of 960 μF and voltage setting of 400 V or an Electo Cell Manipulator 600 (BTX) at settings of 200, 225, or 275 μF, 475 V and R10 as described elsewhere (Potenza et al., 1992; Graminski et al., 1993; McClintock et al., 1993). Using the Bio-Rad apparatus, 40 μg of plasmid DNA was electroporated into 2×10^6 cells in a volume of 800 μl in a 0.4 cm gap cuvette, and using the BTX apparatus, 10 or 20 μg of plasmid DNA was electroporated into 0.5×10^6 cells in a volume of 200 μl in a 0.2 cm gap cuvette. For the cAMP assays, 40 μg of plasmid DNA were electroporated into 5×10^6 cells in a volume of 400 μl in a 0.2 cm gap cuvette using the BTX apparatus set at a capacitance of 400 μF. Cells were seeded into Cell-Tak–coated (Collaborative Research Incorporated) wells in tissue culture plates or dishes (Falcon or SLT/Tecan) as Cell-Tak allowed for better cell attachment and survival following electroporation. Cells were assayed 3 d following electroporation. Transfection efficiency was routinely assayed by *in situ* staining for β-galactosidase activity of cells transfected with a *lacZ*-encoding plasmid as described previously (Lim and Chae, 1989; Potenza and Lerner, 1991). D_2R-expressing melanophores were generated by transfecting with a 1:30 (see Figs. 4, 5, 8; Tables 1, 2) or a 1:100 (see Fig. 7) weight-to-weight mixture of the D_2R-encoding pJGD2R and the *lacZ*-encoding pJG3.6lacz, and D_3R-expressing melanophores were generated by transfecting with either a 1:10 (see Figs. 6, 7; Tables 1, 2) weight-to-weight mixture of the D_3R-encoding pRC/CMV construct and the *lacZ*-encoding pJG3.6lacz or undiluted D_3R-encoding pRC/CMV construct (see Fig. 8). The term "mock-transfected" is used to describe melanophores electroporated with pJG3.6lacz or a 1:20 or 1:30 weight-to-weight mixture of the pcDNAI/NEO and the *lacZ*-encoding pON260. No differences in response were noted for D_3R-expressing cells transfected with either undiluted D_3R-encoding plasmid or a 1:10 or 1:30 weight-to-weight dilution with noncoding plasmid, and D_3R-expressing melanophores transfected with a 1:100 mixture responded to dopaminergic agonists with similar potency but decreased efficacy in the pigment aggregation assay (data not shown).

Computer-enhanced video microscopy. Directly digitized images were obtained using a Videk camera operated via a Macintosh FX computer and analyzed as described previously (McClintock et al., 1993).

Results

Selection of an appropriate pigment dispersing stimulus for use in a pigment aggregation assay. When employing pigment aggregation as a signal for ligand-mediated activation of G_iRs in melanophores, it is useful to set the cells in an initial state of pigment dispersion. The following criteria were considered when selecting an appropriate method for achieving melanosome dispersion. The pigment dispersed state should be (1) non- or slowly desensitizing, (2) maximal (i.e., melanosomes extending to the cell periphery), and (3) "reversible," meaning that ligand-mediated activation of a G_iR should produce pigment aggregation in the continued presence of the pigment-dispersing agent. Conveniently, *Xenopus laevis* melanophores have an endogenous photoreceptor, which, when activated, promotes cAMP accumulation and pigment dispersion (Daniolos et al., 1990). White light at approximately 1.2 mW/cm^2 was found to provide an ideal means for presetting the cells to assess agonist-induced melanosome aggregation. When exposed for 30 min to light of this intensity, the melanophores disperse their pigment (see Fig. 2*A*) but do not accumulate measurable quantities of cAMP [60 pmol/mg as compared to the "basal" level of 50–90 pmol/mg in melatonin-treated cells (Potenza and Lerner, 1992; Potenza et al., 1992; Graminski et al., 1993)]. This level of photostimulation produces melanosome dispersion which persists for at least several hours (see Fig. 3*A*).

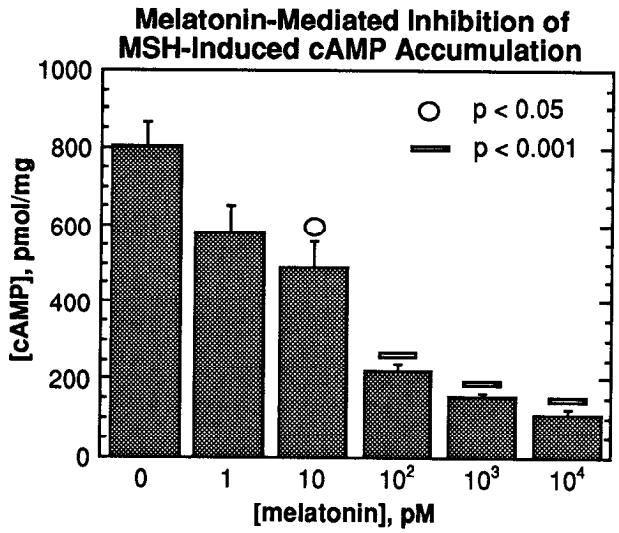

Figure 1. Dose-dependent inhibition of intracellular cAMP accumulation by melatonin. cAMP was extracted from cells incubated in the dark for 30 min in the presence of 100 nM MSH and the indicated concentrations of melatonin. Values are the averages obtained from triplicate samples, with error bars representing the corresponding SEMs. Significance of values with respect to that for the "no drug" sample was determined by two-tailed *t* tests, and the corresponding *p* values are displayed.

Melatonin-induced pigment aggregation. The melatonin receptor, characterized in melanophores as inducing ligand-mediated inhibition of AC (Abe et al., 1969), was initially studied to optimize the conditions and determine the validity of assessing pigment aggregation for the analysis of G_iRs. When applied to the cultured melanophores, melatonin was shown to induce a dose-dependent decrease in MSH-mediated intracellular cAMP accumulation (Fig. 1), with an EC_{50} between 10 and 100 pM. This value correlates with the K_D of 59 pM determined for the binding of radiolabeled melatonin upon membranes isolated from the same cell line of melanophores (S. Reppert, personal communication).

The pigment aggregation that occurs within the melanophores during incubation with melatonin is shown in Figure 2. Figure 2*A* shows a digital video image of melanophores after 30 min of exposure to white light, and Figure 2*B* shows the same field of cells 30 min after incubation with melatonin at a concentration of 10 nM in the continued presence of light. In Figure 2*C*, computer-enhanced video subtraction was used to highlight areas in which pigment aggregation has occurred by the application of green pseudocolor (McClintock et al., 1993). A subtracted image of a similar field of melanophores receiving the same photostimulation and no melatonin is included for comparison (Fig. 2*D*). The results demonstrate that ligand-mediated stimulation of a G_iR can be monitored by melanosome aggregation in photostimulated melanophores.

Quantitation of ligand-mediated stimulation of a G_iR in a microtiter-based assay. The equation $A_r/A_t - 1$ is employed to

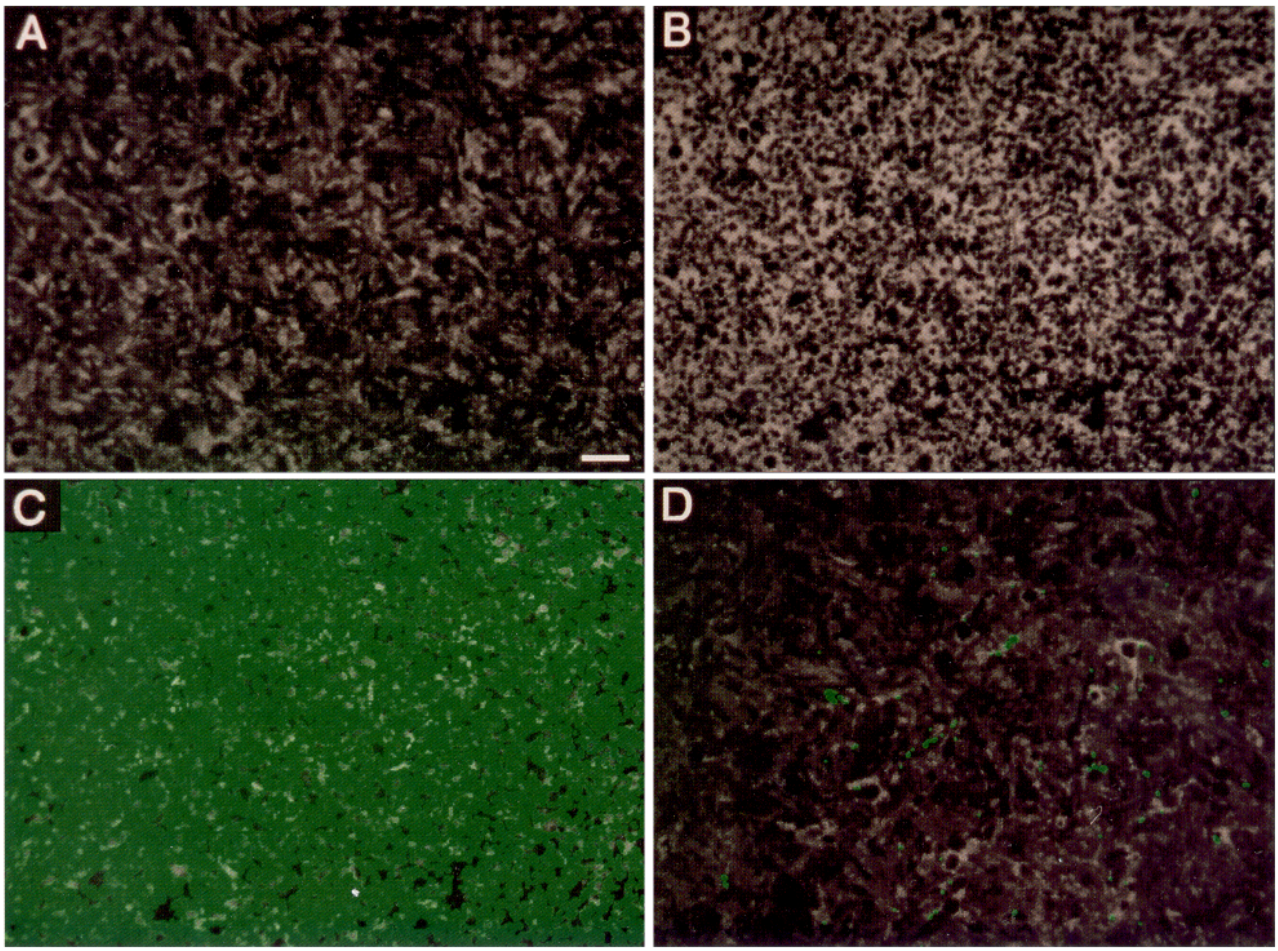

Figure 2. Visualization by computer-enhanced image subtraction of melatonin-induced pigment aggregation within individual melanophores. Three days following their seeding into the Cell-Tak–coated wells of a 24-well tissue culture plate, melanophores were exposed to white light at 1–1.4 mW/cm² for 30 min. A directly digitized image of the cells was obtained immediately (*A*) and 30 min following (*B*) addition of melatonin to 10 nM in the continued presence of light. An image that highlights areas of pigment aggregation (*C*) was created by subtracting the image in *B* from that in *A*, applying green pseudocolor to areas in which gray scale values changed by 10% or greater, and overlaying the pseudocolor bitmap onto the image displayed in *B*. An image processed as that in *C* is displayed (*D*), and it demonstrates the lack of pigment aggregation in cells receiving the same photostimulation and no melatonin. Scale bar, 200 μm.

quantitate melanosome aggregation. In this equation, A_I represents the initial absorbance of 620 nm light by cells, and A_F the absorbance at selected times following drug addition. The term $A_F/A_I - 1$ produces a value of zero for no change in absorbance and decreasing values with a minimum of negative one for decreasing absorbance secondary to pigment aggregation. Because A_I is comparably large, it provides for a reliable intrawell standard.

Using the conditions and equations described above, melatonin-induced pigment aggregation was measured. As described in Materials and Methods, melanophores seeded into standard tissue culture microtiter plates were exposed to white light to stimulate melanosome dispersion, and then varying concentrations of melatonin were added in the continued presence of the light. Figure 3*A* displays the dose-dependent, agonist-induced pigment aggregation over a 4 hr time course. Several properties of the assay are apparent from analysis of the figure. First, examination of early time point values for the "no drug" samples reveals there exists a small (generally −0.02 to −0.10 units) decrease in $A_F/A_I - 1$ upon drug addition. This decrease was determined not to be due to pigment aggregation, but rather to the 50 μl of Excell medium in which the drugs were added (data not shown). Second, $A_F/A_I - 1$ values for the no drug samples rise gradually during the experiment. This increase probably represents a small amount of continued pigment dispersion, as some melanophores (≤2%) do not completely disperse their pigment following a 30 min exposure to 1–1.4 mW/cm² of white light. For these reasons, values in the following graphs are presented as $\Delta(A_F/A_I - 1)$, in which the corresponding no drug value is subtracted from the experimental value. Third, and most importantly, ligand/receptor-mediated responses can be rapidly and accurately monitored over time. High concentrations of melatonin produce maximal pigment aggregation by approximately 2 hr, and this state remains constant for at least an additional 2 hr. Low concentrations of the drug, however, produce pigment aggregation that peaks at earlier times and at lower absolute values of $A_F/A_I - 1$. Although the reasons for pigment redispersion following application of intermediate doses of melatonin have not been fully explored, non-mutually-exclusive possibilities include drug degradation or sequestration, receptor desensitization or sequestration, and low level cAMP accumulation upon prolonged exposure to light.

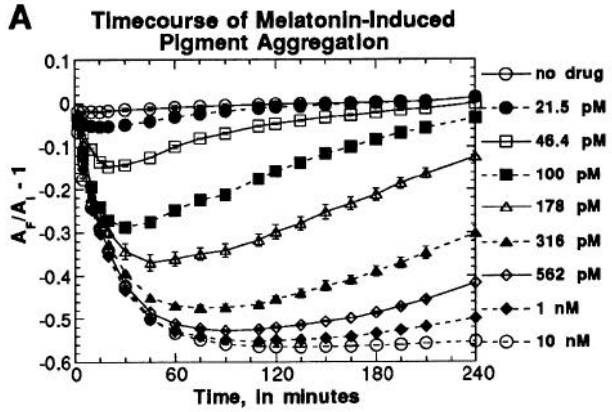

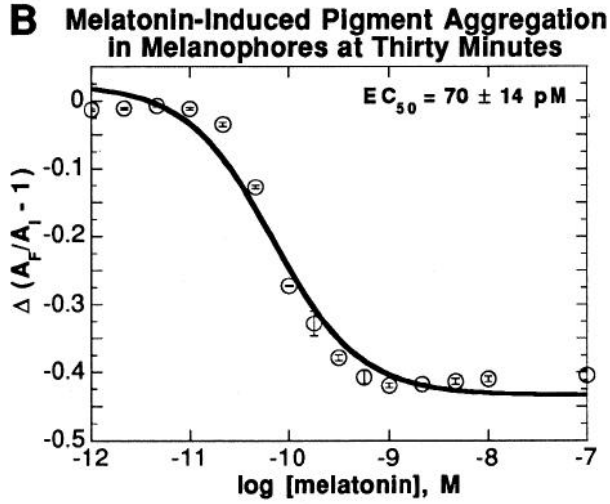

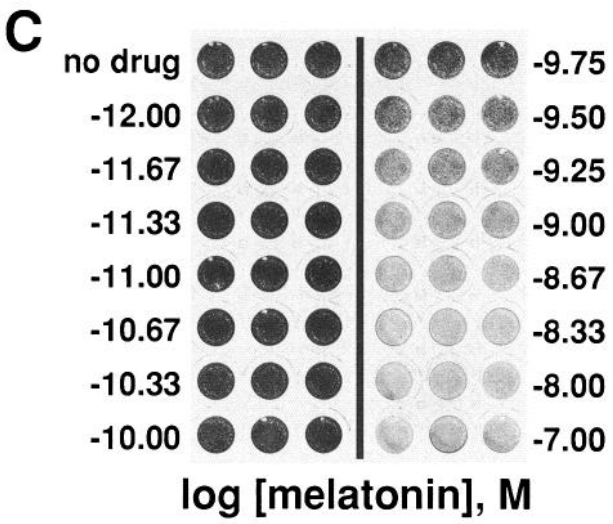

Figure 3. Quantitation of melatonin-induced pigment aggregation. Melanophores seeded into 96-well tissue culture plates at 30,000 cells per well were assayed on the third day following plating, as described in Materials and Methods. Melanophores with pigment dispersed by exposure to white light for 30 min were incubated with the indicated concentrations of melatonin in the continued presence of white light. The changes in absorbance over time (*A*) or at 30 min (*B*) are displayed. At the end of the 4 hr incubation, the cells were fixed in 70% ethanol, and a photograph of the triplicate wells, corresponding to the final time point in *A*, is presented (*C*). In *A* and *B*, values are the averages obtained from triplicate samples, with error bars representing the corresponding SEMs. The data in *B* are curve-fit as defined in Materials and Methods.

By plotting the data in Figure 3*A* in a different fashion, dose response curves at any timepoint can be generated. For example, if $\Delta(A_F/A_I - 1)$ values for samples exposed to varying concentrations of melatonin for 30 min are plotted versus log[melatonin] (Fig. 3*B*), the data can be approximated by a curve defined by an equation that describes a simple equilibrium, as has been described elsewhere for PLC-mediated pigment dispersion in melanophores (Graminski et al., 1993). However, the curve is not quite as steep as one produced by connecting the data points. Contributory factors for this finding might include the high cell density that could mask the "onset" of the response and/or the fact that the pigment aggregation response is dependent upon a signal transduction cascade and not merely ligand/receptor interaction. To determine whether cell density would alter EC_{50} value determinations, melanophores were seeded at varying densities (10,000, 15,000, 20,000, or 30,000 cells per well) and examined as were the samples in Figure 3, *A* and *B*. Although lower peak absolute values of $\Delta(A_F/A_I - 1)$ with greater SEMs were obtained for wells with fewer cells, the shapes of the curves and EC_{50} values were virtually unchanged (data not shown). The EC_{50} value of 70 pM determined from the data displayed in Figure 3*B* is in good agreement with that determined for the inhibition of intracellular cAMP accumulation and the K_D for radiolabeled melatonin binding (see above). The EC_{50} value is somewhat time dependent, with time points later than 30 min producing greater EC_{50} values due to pigment redispersion (see Fig. 3*A*). A photograph of the microtiter plate employed for the generation of data in Figure 3, *A* and *B*, is shown in Figure 3*C*. It provides a visual equivalent of the 4 hr time point in Figure 3*A*. The data presented in Figure 3 demonstrate that the microtiter-based melanophore pigment aggregation assay allows for the rapid and accurate generation of time course analyses, dose–response curves, and EC_{50} value determinations for ligand-mediated stimulation of a G_iR endogenous to the melanophores.

Functional expression of a human D_2R in Xenopus *melanophores.* To determine whether the melanophores could functionally express G_iRs not endogenous to the cells, a D_2R was chosen for initial experimentation (Bunzow et al., 1988; Dal Toso et al., 1989; Grandy et al., 1989; Civelli et al., 1991; Sibley and Monsma, 1992). Transient expression of the D_2R in the melanophores was monitored by computer-enhanced videography (Fig. 4). Images of D_2R-expressing (Fig. 4*A–D*), mock-transfected (*E*), and WT (*F*) melanophores were obtained and processed in a manner similar to those in Figure 2. The top set of images (Fig. 4*A–C*) displays the same field of cells. In the first panel, D_2R-expressing melanophores with their pigment granules dispersed by white light were exposed to 100 nM (−)-quinpirole for 30 min in the continued presence of light. Cells that aggregated their pigment during the incubation are highlighted with green pseudocolor by subtractive videography (Fig. 4*A*). In the continued presence of light and (−)-quinpirole, 1 μM spiperone, a potent and selective D_2R antagonist, was ap-

plied to the cells. Melanophores that dispersed their pigment during incubation with spiperone are highlighted with red pseudocolor (Fig. 4*B*). By overlaying the color bitmaps displayed in Figure 4, *A* and *B*, a twice-subtracted image can be constructed in which cells aggregating and redispersing their pigment during the incubations with (−)-quinpirole and spiperone, respectively, are colored yellow (*C*). A similarly prepared twice-subtracted image of D_2R-expressing melanophores receiving the identical photostimulation as the cells in Figure 4*A–C*, but no (−)-quinpirole or spiperone, shows no yellow coloration (*D*). Likewise, twice-subtracted images of mock-transfected (Fig. 4*E*) or WT (*F*) cells treated identically as those in *A–C* reveal no evidence of a response to the D_2R agonist and antagonist. These results demonstrate that expression of a human D_2R in the melanophores allows for D_2R-selective agonist- and antagonist-induced pigment aggregation and redispersion, respectively.

Quantitation of the effects of agonists upon the D_2R. Dopaminergic agonists were tested for their effects upon D_2R-expressing cells (Fig. 5*A,B*). The time courses of pigment aggregation in D_2R-expressing melanophores in response to varying concentrations of 7-OH DPAT is shown (Fig. 5*A*). In contrast to WT cells, the D_2R-expressing ones exhibit increasing degrees of pigment aggregation upon incubation with increasing concentrations of drug. Provided for comparison is the response of the D_2R-expressing cells to melatonin. The data demonstrate that the pigment aggregation response initiated by 1 μM 7-OH DPAT approaches that induced by 10 nM melatonin, reflecting the high rate of transient transfection (ca. 75–90% by single cell analysis and *in situ* β-galactosidase staining, data not shown). Shown in Figure 5*B* are the responses at 30 min to TNPA [*R*(−)2,10,11-trihydroxy-*N*-propylnoraporphine hydrobromide], a dopaminergic drug that binds to D_2Rs with high affinity (Gao et al., 1990), and bromocryptine, another D_2R-selective agonist (Fluckinger and Wagner, 1968). In contrast to the mock-transfected cells, the D_2R-expressing melanophores exhibit dose-dependent pigment aggregation in response to both drugs. A list of EC_{50} values for the dopaminergic agonists tested upon D_2R-expressing melanophores is shown (Table 1). These EC_{50} values are in general agreement with those previously described. For example, (±)-quinpirole (LY 141,865) produced D_2R-mediated inhibition of prolactin release from isolated rat pituitary with an IC_{50} value of 8.8 nM (Ruffolo and Shaar, 1983), and incubation of D_2R-expressing melanophores with (−)-quinpirole, the more active enantiomer, produced dose-dependent pigment aggregation with an EC_{50} value of 10.9 ± 3.1 nM (Table 1). The rank order potency for these agonists, as determined using the melanophore-based assay, also follows previously described results: TNPA (Gao et al., 1990) is the most potent of the agonists tested and SKF 38,393, the D_1R-selective agonist (Kaiser et al., 1982; Sibley et al., 1982), the least potent. Further, the rank order potency of bromocryptine > dopamine > (+)3-PPP [(3-hydroxyphenyl)-*N*-1-propylpiperidine] is identical to that reported elsewhere for murine fibroblasts expressing a rat D_2R (Neve et al., 1989). Therefore, although minor discrepancies are sometimes observed when expressing receptors in different cellular environments, especially in transient expression systems in which receptor number per cell varies, the expression of the D_2R in the melanophores allows for rapid determinations of reliable EC_{50} values and rank order potencies for dopaminergic agonists upon the receptor.

Quantitation of the effects of antagonists upon the D_2R. By coincubating the D_2R-expressing melanophores with varying concentrations of dopaminergic antagonists and a fixed concentration of agonist, the microtiter-based pigment aggregation assay can be employed to evaluate antagonists (Fig. 5*C,D*). The time course of pigment aggregation initiated by 30 nM (−)-quinpirole and varying concentrations of (±)-sulpiride, a D_2R-selective antagonist, is displayed (Fig. 5*C*). As expected, (±)-sulpiride blocks (−)-quinpirole–induced pigment aggregation in a manner that is both time and dose dependent.

Interestingly, high concentrations of (±)-sulpiride produce positive $\Delta(A_f/A_i - 1)$ values. While the actual reason for pigment dispersion in response to the antagonist is unknown, it could be explained by the D_2R-expressing melanophores having a population of activated receptors in the absence of dopaminergic ligands. Circumstantial evidence supporting this notion comes from several observations. First, the majority of D_2R-expressing melanophores, unlike WT or mock-transfected cells, have their pigment tightly aggregated when they are initially removed from the darkness in the incubator after storage overnight in serum-free medium (data not shown). Second, upon overnight incubation with PTX at 1 μg/ml, D_2R-expressing cells do not have their pigment aggregated, but rather all cells have their pigment dispersed (see below). Third, the intensity and duration of photostimulation used in the pigment aggregation assay are not sufficient to induce pigment dispersion within every D_2R-expressing melanophore. This property is different from those exhibited by WT or mock-transfected cells, in which 30 min of photostimulation elicits pigment dispersion within virtually all of the melanophores. Fourth, the first and third observations are dependent upon the degree of dilution of D_2R-encoding plasmid into carrier plasmid (generally encoding *lacZ*) employed during transfection. That is, upon electroporating the melanophores with undiluted D_2R-encoding plasmid and assaying for pigment translocation by video imaging, the majority of cells do not disperse their pigment in response to photostimulation but will do so upon incubation with a dopaminergic antagonist in the continued presence of light (data not shown). Therefore, it appears that the number of receptors expressed by the cells, which can in part be controlled by limiting the number of receptor-encoding plasmids entering the cell (McClintock et al., 1993), contributes to the response of the transfected cells. General equilibrium equations predict that a small number of receptors are in the active conformation in the absence of ligand, and that high level expression of a GR, expected for a gene under the transcriptional regulation of the CMV promoter, might allow for intrinsic G-protein stimulation and initiation of an appropriate signal transduction cascade. Consistent with this notion is the previously described robust interaction of the D_2R with G-proteins in other systems (Levesque et al., 1992; Sokoloff et al., 1992). The finding that pigment distribution facilitates the direct visualization of receptor function is testimony to the sensitivity of its use as a signal for G_iR activation.

Dose–response curves at 30 min for the racemic mixture and the less active enantiomer of sulpiride are shown (Fig. 5*D*). As expected, (±)-sulpiride has an approximately 50-fold greater potency. When the data points are fit to a curve defined by a simple equilibrium equation, IC_{50} values of 13.0 nM and 640 nM are generated for the (±) and (+) forms, respectively. The rank order potency of the antagonists tested [spiperone > (±)-sulpiride > (+)-sulpiride > SCH 23,390] is that predicted from binding studies described elsewhere (Seeman and Niznik, 1988). Also, none of the D_2R antagonists tested produced measurable pigment dispersion in WT cells preset with 1 nM melatonin in

Table 1. EC_{50} valves of drugs upon human D_2R and D_3R as determined using the pigment aggregation assay

Agonist	Class	EC_{50} (nM) D_2R	D_3R
TNPA	Potent D_2R-selective	1.54 ± 0.32	1.44 ± 0.43
(−)-Quinpirole	"$D_3R > D_2R$-selective"	10.9 ± 3.1	15.4 ± 3.82
Bromocryptine	D_2R-selective	24.5 ± 9.52	43.5 ± 16.9
7-OH DPAT	"$D_3R > D_2R$-selective"	56.2 ± 13.2	113 ± 49
Dopamine	Endogenous	154 ± 101	295 ± 240
(+)-3 PPP	Autoreceptor, postsynaptic	1103 ± 396	1102 ± 129
SKF 38,393	D_1R-selective	≫1000	≫1000

The values listed are representative of duplicate to quintuplicate experiments using triplicate samples for each concentration as displayed and described in figures and their captions.

the pigment dispersion assay (data not shown). These results demonstrate that the pigment aggregation assay can be employed for the rapid evaluation of IC_{50} values and rank order potencies of antagonists upon the D_2R.

Functional expression of a human D_3R in the melanophores. The demonstration of the feasibility of the microtiter-based pigment aggregation assay for the pharmacological characterization of a human D_2R suggested it could be used to study a human D_3R. The D_3R, like the D_2R and the D_4R, belongs to the D_2R-like subfamily of DRs, which are characterized by extensive sequence similarity, structural relatedness (in terms of presence and distribution of introns), and ligand-binding profiles (Giros et al., 1990; Sokoloff et al., 1990; Civelli et al., 1991; Van Tol et al., 1991; Sibley and Monsma, 1992). When expressed in the melanophores, the D_3R enabled the melanophores to aggregate their pigment in response to dopaminergic agonists (Fig. 6, Table 1). Shown in Figure 6*A* is the time course of pigment aggregation in response to 7-OH DPAT, a drug reported to bind to the D_3R with approximately 100-fold selectivity over the D_2R in another system (Levesque et al., 1992). Like the D_2R-expressing melanophores, D_3R-expressing melanophores exhibit time- and dose-dependent pigment aggregation in response to 7-OH DPAT. Analysis of the data reveals that although high concentrations of 7-OH DPAT produce similar $\Delta(A_F/A_I - 1)$ values when applied to melanophores expressing either DR, the relative degree of 7-OH DPAT–induced pigment aggregation, as compared with that elicited by melatonin, is lower in the case of the D_3R-expressing melanophores (see Figs. 5*A*, 6*A*). The absolute degree of change in the value of $\Delta(A_F/A_I - 1)$ is dependent on several factors: cell density, state of pigment distribution at time zero, and number of responding cells (which itself is dependent upon transfection efficiency). The time course analyses shown in Figures 5*A* and 6*A* were performed simultaneously using cells plated at approximately equal densities, and the D_2R- and D_3R-expressing cells displayed approximately equal rates of transient transfection as determined by *in situ* β-galactosidase staining (data not shown). Unlike the D_2R-expressing melanophores, the D_3R-expressing ones are not tightly pigment aggregated upon incubation in the dark and they disperse their pigment maximally upon photostimulation similarly to WT or mock-transfected cells (data not shown). In other words, with respect to the D_2R-expressing cells, a greater percentage of the D_3R-expressing cells have their pigment dispersed at the onset of the time course analyses. Therefore, when plated at similar densities, the D_3R-expressing cells can produce a greater change in absolute pigment aggregation, as demonstrated by their response to 10 nM melatonin. Consequently, the response of the D_3R-expressing cells to high concentrations of 7-OH DPAT is relatively weaker than the corresponding response elicited in the D_2R-expressing cells. The underlying cause for a less efficacious pigment aggregation response to D_3R activation compared with D_2R stimulation is unknown. However, the observations are consistent with previous reports documenting the weaker ability of the D_3R to interact with G-proteins in a mammalian expression system (Levesque et al., 1992; Sokoloff et al., 1992).

Although the magnitude of response of D_3R-expressing melanophores differs from their D_2R-expressing counterparts, the concentration of agonist needed to induce pigment aggregation is similar. The dose responses at 30 min to (−)-quinpirole and corresponding to EC_{50} values are shown (Fig. 6*B*, Table 1). Each of the seven agonists tested displayed similar EC_{50} values and identical rank order potencies upon the two dopaminergic receptors. Although this result is consistent with the pharmacological and structural similarities of the receptors, it was unanticipated for several of the ligands, such as (−)-quinpirole and

Table 2. IC_{50} values of drugs upon human D_2R and D_3R as determined using the pigment aggregation assay

Antagonist	Class	IC_{50} (nM)[a] D_2R	D_3R
Spiperone	D_2R-selective	4.97 ± 7.24	328 ± 172
(±)-Sulpiride	D_2R-selective	13.0 ± 2.45	999 ± 258
(+)-Sulpiride	Less active enantiomer	640 ± 59	46,700 ± 22,300
SCH 23,390	D_1R-selective	>10,000	>10,000

The values listed are representative of duplicate to quadruplicate experiments using triplicate samples for each concentration as displayed and described in the figures and their captions.

[a] The values were determined in the presence of 30 nM (−)-quinpirole.

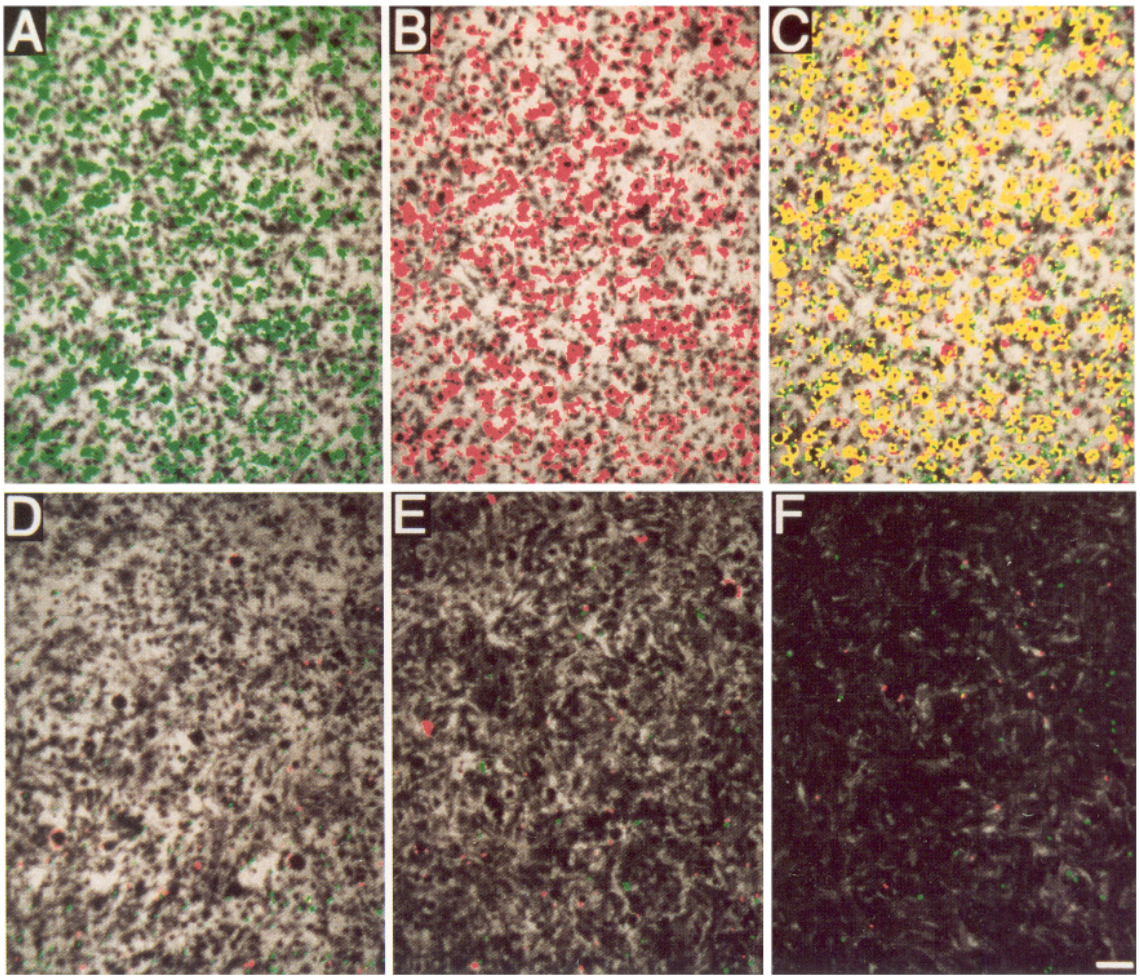

Figure 4. Visualization by computer-enhanced image subtraction of (−)-quinpirole–induced pigment aggregation and spiperone-induced pigment dispersion within individual D_2R-expressing melanophores. D_2R-expressing (*A–D*), mock-transfected (*E*), or WT (*F*) melanophores were exposed to white light for 30 min, incubated with 100 nM (−)-quinpirole for 30 min in the continued presence of light, and incubated with 1 μM spiperone in the continued presence of (−)-quinpirole and light for 30 min. Subtracted images of D_2R-expressing melanophores highlight cells that have aggregated their pigment during incubation with (−)-quinpirole (*green* in *A*) and dispersed their pigment during incubation with spiperone (*red* in *B*). The overlaying of the color bitmaps in *A* and *B* produces a twice-subtracted image in which *yellow* corresponds to (−)-quinpirole–induced aggregation and spiperone-induced dispersion (*C*). The twice-subtracted image of D_2R-expressing melanophores exposed to the identical photostimulation in the absence of (−)-quinpirole and spiperone is displayed for comparison (*D*), as are those of β-galactosidase–expressing (*E*) or WT (*F*) melanophores treated as were the cells in *A–C*. Scale bar, 200 μm.

7-OH DPAT. These two ligands display approximately 30- and 100-fold higher affinity, respectively, for the D_3R in other systems (Levesque et al., 1992; Sokoloff et al., 1992). It is interesting that in the melanophore system the EC_{50} values for agonists tested to activate functionally the D_2R and D_3R are similar. The results demonstrate that the pigment aggregation assay can be used for the rapid evaluation of ligands upon the D_3R.

Quantitation of the effects of antagonists upon the D_3R. To analyze further the function of the D_3R, dopaminergic antagonists were tested for their abilities to block (−)-quinpirole–induced pigment aggregation (Fig. 6, Table 2). Antagonism was found to be both time and dose dependent, and the rank order potency of spiperone > (±)-sulpiride > (+)-sulpiride > SCH 23,390 is the same observed upon the D_2R. One striking difference was the finding that each of the antagonists displaying an ability to block (−)-quinpirole–induced pigment aggregation was approximately 70-fold less potent upon the D_3R than upon the D_2R. In contrast, the active enantiomer of sulpiride has been shown to bind D_2Rs and D_3Rs with approximately equal affinities (Levesque et al., 1992; Sokoloff et al., 1992). The underlying reason for the difference has not been fully explored, although differences in binding of (−)-quinpirole to the two receptors may be responsible (Sokoloff et al., 1992).

PTX inhibits agonist-induced pigment aggregation in D_2R- and D_3R-expressing melanophores. The finding that the D_3R can induce pigment aggregation in the melanophores suggests it might couple to the inhibition of AC. In order to examine this possibility, studies employing PTX were undertaken. PTX catalyzes the ADP-ribosylation of a specific cysteine residue near the carboxy terminus in members of the $G\alpha_i$ family (Katada and Ui, 1981, 1982; West et al., 1985). In doing so, PTX renders the Gα subunit incapable of proper signal transduction. To verify the suitability of using PTX to examine the function of the dopamine receptors in the melanophores, the effects of the drug were first tested upon the WT cells (Fig. 7*A,B*). Shown in Figure 7*A* is the time course of melatonin-induced pigment aggregation

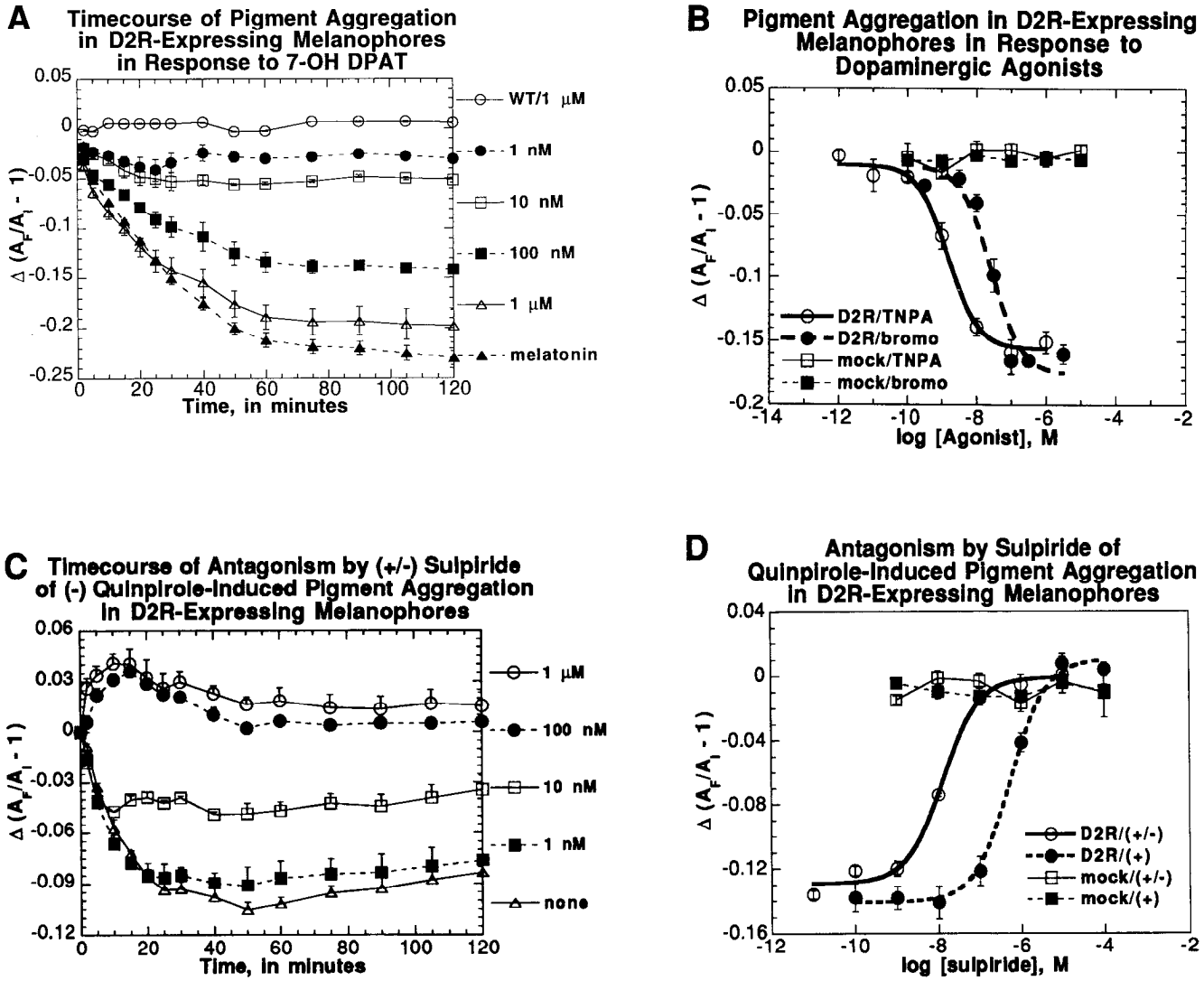

Figure 5. Quantitation of ligand-mediated stimulation and blockade of the D_2R transiently expressed in *Xenopus* melanophores. WT, mock-transfected, and D_2R-expressing melanophores were tested in a microtiter plate assay as described in Materials and Methods. The time course of pigment aggregation in D_2R-expressing and WT melanophores in response to 7-OH DPAT is shown (*A*). The WT cells were treated with 1 μM 7-OH DPAT, and the concentration of melatonin applied to the D_2R-expressing cells was 10 nM. Dose–response curves at 30 min for the dopaminergic agonists TNPA and bromocryptine upon D_2R-expressing or WT cells are displayed (*B*). WT, mock-transfected, and D_2R-expressing melanophores were tested in a microtiter plate assay as described in Materials and Methods. The time course of pigment aggregation in D_2R-expressing melanophores in response to 30 nM (−)-quinpirole and various concentrations of (±)-sulpiride is shown (*C*). Dose–response curves at 30 min for the inhibition of (−)-quinpirole–induced pigment aggregation in D_2R-expressing melanophores by the dopaminergic antagonists (±)- and (+)-sulpiride are displayed (*D*). Values are the averages of triplicate samples, with error bars representing the corresponding SEMs.

in melanophores incubated overnight in different concentrations of PTX. Consistent with previous reports (Sugden, 1991), increasing concentrations of PTX increasingly retard the melanosome aggregation induced by 1 nM melatonin. Similar results were obtained by stimulating the cells with 10 nM or 100 nM melatonin, and some of these data are presented as dose–response curves (Fig. 7*B*).

The effects of PTX were next examined upon D_2R-expressing (Fig. 7*C,D*) and D_3R-expressing (Fig. 7*E,F*) melanophores. In both cases, incubation with increasing concentrations of PTX produced greater losses in the ability of the DR-expressing cells to aggregate their pigment in response to (−)-quinpirole. Interestingly, a higher concentration of PTX is needed to block the (−)-quinpirole–induced pigment aggregation in the DR-expressing cells than is required to retard the melatonin-induced pigment aggregation in the WT cells. Three explanations for the difference in sensitivity to PTX include the possibilities that (1) different G-proteins are employed by the DRs and the melatonin receptor, (2) expression of the DRs in the melanophores alters the expression of particular G-proteins, and (3) the DRs can more efficiently recruit the remaining active Gα subunits involved in the signal transduction cascade culminating in pigment aggregation. Regardless of the minor differences in PTX sensitivity observed, the finding that pigment aggregation mediated by the D_2R and the D_3R is sensitive to PTX supports the concept that each receptor produces its effects via a G_i-protein.

7-OH DPAT initiates inhibition of MSH-induced cAMP accumulation in melanophores expressing either the D_2R or the D_3R. The findings that the D_3R can mediate ligand-activated and PTX-

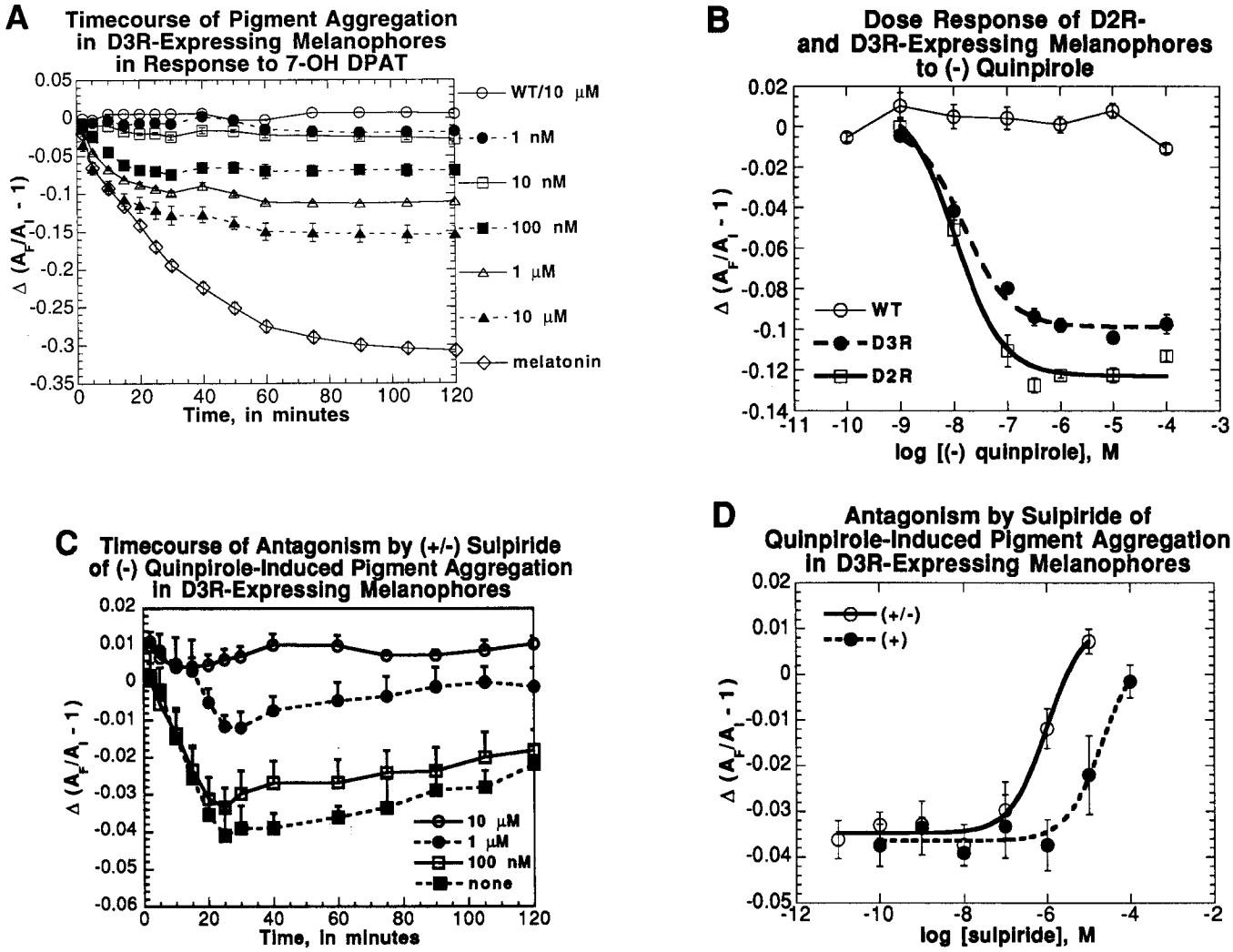

Figure 6. Quantitation of ligand-mediated stimulation and blockade of the D_3R transiently expressed in *Xenopus* melanophores. WT, mock-transfected, D_2R-expressing, and D_3R-expressing melanophores were tested in a microtiter plate assay as described in Materials and Methods. Pigment aggregation response over time of D_3R-expressing and WT melanophores to 7-OH DPAT is shown (*A*). The WT cells were treated with 10 μM 7-OH DPAT, and the concentration of melatonin applied to the D_3R-expressing cells was 10 nM. Dose–response curves at 30 min for the dopaminergic agonist (−)-quinpirole upon D_3R-expressing, D_2R-expressing, or WT cells are displayed (*B*). As in Figures 5*A* and 6*A*, the D_3R-expressing melanophores produced a more robust pigment aggregation response to 10 nM melatonin than did the D_2R-expressing cells. The time course of pigment aggregation in D_3R-expressing melanophores in response to 30 nM (−)-quinpirole and various concentrations of (±)-sulpiride is shown (*C*). Dose–response curves at 30 min for the inhibition of (−)-quinpirole–induced pigment aggregation in D_2R-expressing melanophores by the dopaminergic antagonists (±)- and (+)-sulpiride are displayed (*D*). Values are the averages of triplicate samples, with error bars representing the corresponding SEMs.

sensitive pigment aggregation in the melanophores suggested that the receptor functions by lowering intracellular levels of cAMP. In order to test this hypothesis, direct cAMP measurements were performed upon D_3R-expressing, D_2R-expressing, and mock-transfected melanophores (Fig. 8). As expected, higher concentrations of the agonist 7-OH DPAT inhibited cAMP accumulation to increasing degrees in the D_3R-expressing melanophores over the range of 10 nM to 10 μM. Specifically, a decrease in intracellular cAMP of approximately 20% was observed at 100 nM (not statistically different from corresponding "no drug" value as determined by two-tailed *t* test, $p > 0.2$), 27% at 1 μM (approaching statistical significance, $0.05 < p < 0.1$), and 35% at 10 μM (statistically significant, $0.02 < p < 0.05$). These results are consistent with the data obtained from the microtiter-based assay (Fig. 6*A*), which show 7-OH DPAT–induced pigment aggregation over the range of 100 nM to 10 μM in the D_3R-expressing cells. A greater absolute response in terms of inhibition of cAMP accumulation would likely be observed if all cells were expressing the D_3R. Under these circumstances lower concentrations of 7-OH DPAT might produce statistically significant results. The sensitivity of the pigment aggregation response and the ability to quantitate it throughout time allow the microtiter-based assay to measure, with respect to the standard radioimmunoassay for cAMP, a *significant* response to a lower concentration of 7-OH DPAT upon transiently transfected cells (compare the responses to 100 nM 7-OH DPAT). Mock-transfected cells show no significant change in intracellular cAMP levels when treated with high concentrations of 7-OH DPAT: the decreases of approximately 5% at 1 μM and 10 μM correspond to $p \gg 0.2$. Similarly, no changes in cAMP levels were observed in WT cells treated with 7-OH

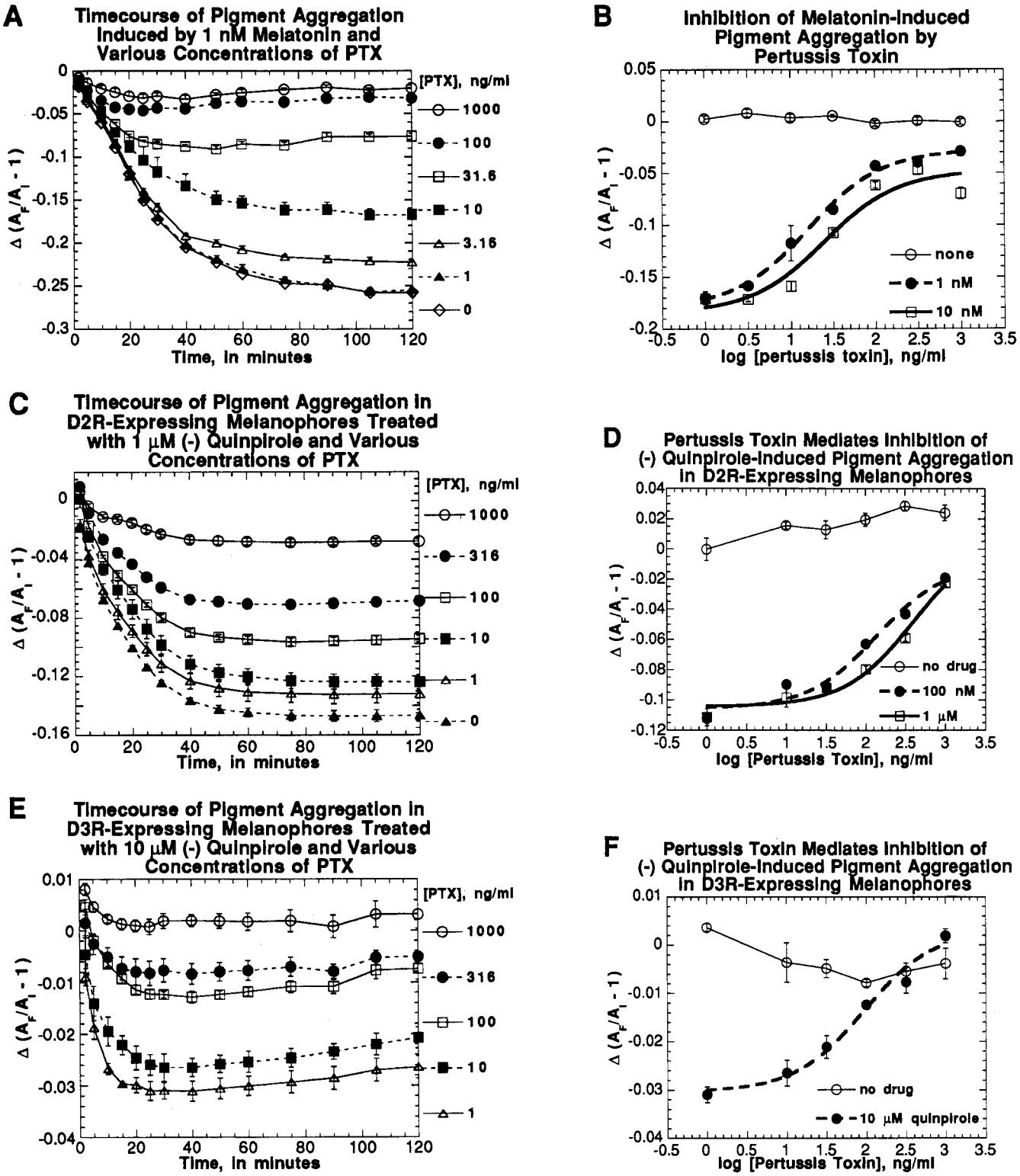

Figure 7. Pretreatment of melanophores with PTX blocks agonist-induced pigment aggregation. WT, D_2R-expressing, and D_3R-expressing melanophores were tested in a microtiter plate assay as described in Materials and Methods. The time course of pigment aggregation in WT melanophores pretreated with different concentrations of PTX in response to 1 nM melatonin is shown (*A*). Dose–response curves at 30 min for the PTX-mediated inhibition of pigment aggregation by 1 nM and 10 nM melatonin are displayed (*B*). The time course of pigment aggregation in D_2R-expressing melanophores in response to 1 μM (−)-quinpirole and various concentrations of PTX is shown (*C*). Dose–response curves at 30 min for pigment aggregation induced by 100 nM and 1 μM (−)-quinpirole in D_2R-expressing melanophores pretreated with different concentrations of PTX are displayed (*D*). The time course of pigment aggregation in D_3R-expressing melanophores in response to 10 μM (−)-quinpirole and various concentrations of PTX is shown (*E*). The dose–response curve at 30 min for pigment aggregation by 10 μM (−)-quinpirole in D_3R-expressing melanophores pretreated with different concentrations of PTX is displayed (*F*). The concentration of PTX in ng/ml is listed in the margin of each time course graph, and the concentration of agonist used in the dose–response graphs is displayed. Values are the averages of triplicate samples, with error bars representing the corresponding SEMs.

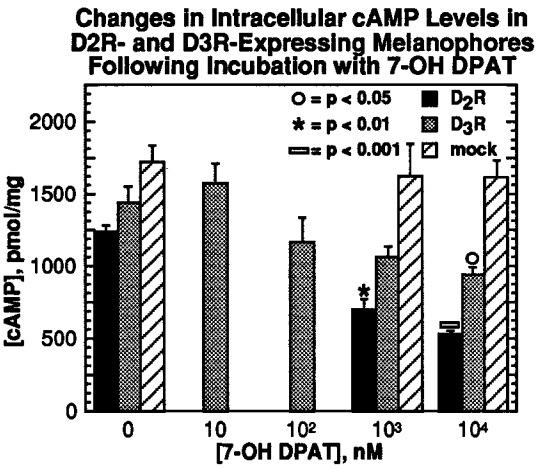

Figure 8. Dose-dependent inhibition of intracellular cAMP accumulation in D_2R-expressing and D_3R-expressing melanophores induced by 7-OH DPAT. cAMP was extracted from D_2R-expressing, D_3R-expressing, and mock-transfected cells incubated in the dark for 30 min in the presence of 100 nM MSH and the indicated concentrations of 7-OH DPAT. Values are the averages obtained from triplicate samples, with error bars representing the corresponding SEMs. Significance of values with respect to the corresponding "no drug" sample value was determined by two-tailed *t* tests, and the corresponding *p* values displayed.

DPAT (data not shown). These results demonstrate that the D_3R, when expressed in the melanophores, functions in a ligand-dependent manner to inhibit cAMP accumulation.

Several interesting observations can be made from comparing the intracellular levels of cAMP in the D_2R-expressing and D_3R-expressing melanophores. First, the D_2R-expressing cells, transfected with a 1:30 weight : weight ratio of D_2R-encoding to carrier plasmid, have a statistically significant lower level of intracellular cAMP than do mock-transfected melanophores in the absence of ligand ($0.02 < p < 0.05$). This 28% decrease is greater than the 16% decrease ($0.1 < p < 0.2$) observed in the D_3R-expressing cells, which were transfected with undiluted D_3R-encoding plasmid. Moreover, the levels of cAMP measured upon stimulation with 7-OH DPAT are significantly lower in the D_2R-expressing cells than in the D_3R-expressing ones (for 1 μM, $0.02 < p < 0.05$; for 10 μM, $0.001 < p < 0.01$). In contrast, the level of cAMP observed upon incubation with 10 nM melatonin was similar in the three cell types: 234.8 ± 29.1 pmol/mg for the D_3R-expressing cells, 251.9 ± 33.3 for the D_2R-expressing ones, and 237.7 ± 25.1 for the mock-transfected melanophores. The results are consistent with previous reports describing the robust association of the D_2R with G-proteins and inhibition of AC (Sokoloff et al., 1992), and the notion discussed above that a population of D_2Rs might be active in the absence of ligand in the melanophores transiently expressing the receptor.

Discussion

The data presented here were obtained with a powerful, melanophore-based bioassay that made possible the rapid quantitation of the effects of dopaminergic agonists and antagonists upon two human DRs. To our knowledge, this is the first report of functional expression of the D_3R that enabled EC_{50} and IC_{50} value determinations to be made. The receptor has been reported to couple only weakly to G-proteins (Levesque et al., 1992; Sokoloff et al., 1992) and, perhaps as a consequence, it was not previously possible to recognize reliable functional activation by receptors (Sokoloff et al., 1992). Analysis of the functional effects of the dopaminergic ligands tested for this report revealed a surprising result; namely, several drugs that have been reported to bind to the D_3R with higher affinity than to the D_2R were shown to have equal potency in terms of their abilities to activate the two receptors. Moreover, while the antagonists tested share the same rank order potencies for the two receptors, each ligand with potency upon the receptors was approximately 70-fold less potent in antagonizing the D_3R as compared to the D_2R. The underlying reason for successful, reliable and quantitatable receptor activation of the D_3R probably represents a combination of the direct visual signal that is the basis of the pigment aggregation assay, the sensitivity of the pigment aggregation response to activation by specific GRs, and the large number of G-protein α-subunits expressed by the melanophores (Karne et al., 1991).

Transient expression of the D_3R in the melanophores also allowed for investigation into potential signaling pathways employed by the receptor. Our findings demonstrate that the agonist-induced pigment aggregation mediated by the D_3R results in the inhibition of intracellular cAMP accumulation and is sensitive to PTX. These results indicate that the D_3R can function via the same second messenger pathway as do the D_2R and D_4R. Interestingly, we observe some day-to-day variation in the magnitude of dopaminergic agonist-induced pigment aggregation in D_3R-expressing melanophores (see Figs. 6, 7), despite obtaining similar transfection rates as determined by *in situ* β-galactosidase staining. This observation is consistent with the report of inconsistent decreases in cAMP levels upon stimulation of the D_3R expressed in Chinese hamster ovary cells (Sokoloff et al., 1992). Although differences in the extent of D_3R-mediated pigment aggregation are seen in different experiments, a quantifiable signal is always obtained. While the underlying reason for the variation remains to be investigated, it is tempting to speculate that the regulation of downstream effectors (e.g., specific G-proteins) is involved. However, it is also possible that some of the observed differences could be attributed to variation in receptor levels, especially as transient transfection was used in the experiments reported here. Further studies, such as investigation of the G-proteins that mediate the signal transduction of the D_3R, are necessary to determine the cause of the observed differences.

The concern always exists with the use of heterologous expression systems that the introduced protein does not function exactly as it does in its native environment. For example, with regard to GRs, one is not certain if the correct G-proteins or other effectors, such as specific isoforms of AC (Glatt and Snyder, 1993), are present in the novel environment. The possibility that the response of the D_3R in the melanophores is artifactual is unlikely with respect to the findings that 14 distinct GRs not normally found in the melanophores have been expressed (including the G_i-linked chick muscarinic 4 and human α_2 adrenergic receptors), and each has appeared to function faithfully in terms of ligand-mediated activation and blockade and second messenger coupling (Potenza et al., 1992; Graminski et al., 1993; McClintock et al., 1993; M. N. Potenza, G. F. Graminski, C. Schmauss, and M. R. Lerner, unpublished observations). Indeed, the melanophores have the potential for the efficient characterization of dopamine receptors in general, as it has been demonstrated that other human DRs, can effect pigment translocation when transiently expressed in the melanophores (M.

N. Potenza, G. F. Graminski, C. Schmauss, G. Petzinger, A. Roby-Shemkovitz, and M. R. Lerner, unpublished observations).

In addition to complementing the previously described melanophore-based bioassays (Potenza and Lerner, 1992; Potenza et al., 1992; Graminski et al., 1993; McClintock et al., 1993), the quantitative, microtiter-based pigment aggregation bioassay should prove useful for the study of G_iRs because it offers many advantages over other functional assays. First, the assay is rapid. Because the agonist-induced, receptor-mediated response does not require transcriptional activation for the generation of its signal, accurate and reproducible measurements of receptor activation or blockade can be made within minutes following incubation of the cells with ligand. Second, the assay relies upon a readily detectable visible response rather than the inhibition of a response, such as in other bioassays used to quantitate ligand-induced G_iR-mediated responses. Third, it does not require killing the cells and consequently facilitates measurements at multiple time points. Fourth, no ligand modification is necessary, and it therefore obviates the problems sometimes encountered during radiolabeling, for example, synthesizing a drug with both high specific activity and binding characteristics representative of its parent compound. Fifth, the assay employs a microtiter-based format readily amenable to automation. Sixth, the assays appears to be more sensitive than a standard RIA for detecting functional activation of G_iRs. For the reasons listed above, the assay appears well suited for the study of G_iRs. We believe the assay will allow for the more efficient investigation of structure/function relationships between ligands and G_iRs, classification of "orphan" G_iRs, and screening of chemicals or mixtures for their potential as agonists or antagonists upon G_iRs. Experiments designed to address these possibilities are in progress.

References

Abe K, Robison GA, Liddle GW, Butcher RW, Nicholson WE, Baird CE (1969) Role of cyclic AMP in mediating the effects of MSH, norepinephrine and melatonin on frog skin color. Endocrinology 85: 674–682.

Bouthenet M-L, Souil E, Martres M-P, Sokoloff P, Giros B, Schwartz J-C (1991) Localization of dopamine D3 receptor mRNA in the rat brain using *in situ* hybridization histochemistry: comparison with D2 receptor mRNA. Brain Res 564:203–219.

Bunzow JR, Van Tol HHM, Grandy DK, Albert P, Salon J, Christi M, Machida CA, Neve KA, Civelli O (1988) Cloning and expression of a rat D_2 dopamine receptor cDNA. Nature 336:783–787.

Caine SB, Koob GF (1993) Modulation of cocaine self-administration in the rat through dopamine D-3 dopamine receptors. Science 260: 1814–1816.

Cheung AH, Huang RR, Graziano MP, Strader CD (1991) Specific activation of G_s by synthetic peptides corresponding to an intracellular loop of the β-adrenergic receptor. FEBS Lett 279:277–280.

Chio CL, Hess GF, Graham RS, Huff RM (1990) A second molecular form of D_2 dopamine receptor in rat and bovine caudate nucleus. Nature 343:266–269.

Civelli O, Bunzow JR, Grandy DK, Zhou Q, Van Tol HHM (1991) Molecular biology of the dopamine receptors. Eur J Pharmacol 207: 277–286.

Coco ML, Kilts CD (1992) Coupling of D3-like receptors to guanine nucleotide binding proteins: a quantitative autoradiography study. Soc Neurosci Abstr 18:1515.

Cohen AI, Todd RD, Harmon S, O'Malley KL (1992) Photoreceptors of mouse retinas possess D_4 receptors coupled to adenylate cyclase. Proc Natl Acad Sci USA 89:12093–12097.

Dahlstrom A, Fuxe K (1964) Evidence for the existence of monoamine-containing neurons in the central nervous system. Acta Physiol Scand 62[Suppl. 232]:1–55.

Dal Toso RS, Ewert M, Herb A, Pritchett DD, Bach A, Shivers BD, Seeburg PH (1989) The dopamine D_2 receptors: two molecular forms generated by alternative splicing. EMBO J 8:4025–4034.

Daniolos A, Lerner AB, Lerner MR (1990) Action of light on frog pigment cells in culture. Pigment Cell Res 3:38–43.

Davis KL, Kahn RS, Ko G, Davidson M (1991) Dopamine in schizophrenia: a review and reconceptualization. Am J Psychiatry 148: 1474–1486.

Dearry A, Gingrich JA, Falardeau P, Fremeau RT Jr, Bates MD, Caron MG (1990) Molecular cloning and expression of the gene for a human D_1 dopamine receptor. Nature 347:72–76.

Fluckinger E, Wagner H (1968) 2-Br-α-Ergokryptin: Beeinflussung von Fertilitat und Laktation bei der Ratte. Experientia 24:1130–1131.

Freedman SB, Patel S, Marwood R, Emms F, Knowles M, Fletcher A, Seabrook G, McAllister G (1992) Pharmacological characterisation of the human D3 receptor. Soc Neurosci Abstr 18:7.

Gao Y, Baldessarini RJ, Kula NS, Neumeyer JL (1990) Synthesis and dopamine receptor affinities of enantiomers of 2-substituted apomorphines and their N-*n* propyl analogues. Am Chem Soc 33:1800–1805.

Giros B, Martres M-P, Sokoloff P, Schwartz J-C (1990) cDNA cloning of the human D_3 dopaminergic receptor and chromosome identification. C R Acad Sci Paris 311:501–508.

Giros B, Martres M-P, Pilon C, Sokoloff P, Schwartz J-C (1991) Shorter variants of the D_3 dopamine receptor produced through various patterns of alternative splicing. Biochem Biophys Res Commun 176: 1584–1592.

Glatt CE, Snyder SH (1993) Cloning and expression of an adenylyl cyclase localized to the corpus striatum. Nature 361:536–538.

Graminski GF, Jayawickreme CK, Potenza MN, Lerner MR (1993) Pigment dispersion in frog melanophores can be induced by a phorbol ester or stimulation of a recombinant receptor that activates phospholipase C. J Biol Chem 268:5957–5964.

Grandy DD, Marchionni MA, Makam H, Stofko RE, Alfano M, Frothingham L, Fischer JF, Burke-Howie KJ, Bunzow JR, Server AC, Civelli O (1989) Cloning of the cDNA and gene for human D_2 dopamine receptor. Proc Natl Acad Sci USA 86:9762–9766.

Guennoun R, Bloch B (1991) D_2 dopamine receptor gene expression in the rat striatum during ontogeny: an *in situ* hybridization study. Dev Brain Res 60:79–87.

Healy D (1991) D_1 and D_2 and D_3. Br J Psychiatry 159:319–324.

Hornykiewicz O (1986) A quarter century of brain dopamine research. In: Dopaminergic systems and their regulation (Woodruff GN, Poat JA, eds), pp 3–18. London: Macmillan.

Huang R-R, Cheung AH, Mazina KE, Strader CL, Fong TM (1992) cDNA sequence and heterologous expression of the human neurokinin-3 receptor. Biochem Biophys Res Commun 184:966–972.

Kaiser C, Dandridge P, Garvey E, Hahn R, Sarau H, Setler P, Bass L, Clardy J (1982) Absolute stereochemistry and dopaminergic activity of enantiomers of 2,3,4,5-tetrahydro-7,8-dihydroxy-1-phenyl-1H-3-benzazepine. J Med Chem 25:697–703.

Kane J, Honigfeld G, Singer J, Meltzer H (1988) Clozapine for the treatment-resistant schizophrenics. Arch Gen Psychiatry 45:789–796.

Karne S, Jayawickreme CK, Nguyen TP, Anderson ML, Lerner MR (1991) Characterization of G-proteins in *Xenopus* melanocytes. Soc Neurosci Abstr 17:607.

Katada T, Ui M (1981) Islet-activating protein; a modifier of receptor mediated regulation of rat adenylate cyclase. J Biol Chem 256:8310–8317.

Katada T, Ui M (1982) Direct modification of the membrane adenylate cyclase by islet-activating protein due to ADP-ribosylation of a membrane protein. Proc Natl Acad Sci USA 79:3129–3133.

Kebabian JW, Greengard P (1971) Dopamine-sensitive adenylyl cyclase: possible role in synaptic transmission. Science 174:1346–1348.

Kebabian JW, Petzold GL, Greengard P (1972) Dopamine-sensitive adenylate cyclase in caudate nucleus of rat brain, and its similarity to the "dopamine receptor." Proc Natl Acad Sci USA 69:2145–2149.

Kubo T, Bujo H, Akiba I, Nakai J, Mishina M, Numa S (1988) Location of a region of the muscarinic acetylcholine receptor involved in selective effector coupling. Fed Eur Biochem Soc 241:119–125.

Lechleiter J, Girard S, Clapham D, Peralta E (1991) Subcellular patterns of calcium release determined by G protein-specific residues of muscarinic receptors. Nature 350:505–508.

Levesque D, Diaz J, Pilon C, Martres M-P, Giros B, Souil E, Schott D, Morgat J-L, Schwartz J-C, Sokoloff P (1992) Identification, char-

acterization, and localization of the dopamine D_3 receptor in rat brain using 7-[^{3}H]hydroxy-*N,N*-di-*n*-propyl-2-aminotetralin. Proc Natl Acad Sci USA 89:8155–8159.

Liggett SB, Caron MG, Lefkowitz RJ, Hnatowich M (1991) Coupling of a mutated form of the human β_2-adrenergic receptor to G_i and G_s. J Biol Chem 266:4816–4821.

Lim K, Chae C (1989) A simple assay for DNA transfection by incubation of the cells in culture dishes with substrates for beta-galactosidase. Biotechniques 7:576–579.

McClintock TS, Graminski GF, Potenza MN, Jayawickreme CK, Roby-Shemkovitz A, Lerner MR (1993) Bioassay of G protein coupled receptor gene expression by video imaging of pigment movement in melanophores. Anal Biochem 209:298–305.

Munch G, Dees C, Hekman M, Palm D (1991) Multisite contacts involved in coupling of the β-adrenergic receptor with the stimulatory guanine-nucleotide-binding regulatory protein. Eur J Biochem 198: 357–364.

Muscat R, Papp M, Willner P (1992) Antidepressant-like effects of dopamine agonists in an animal model of depression. Biol Psychiatry 31:937–946.

Neve KA, Henningsen RA, Bunzow JR, Civelli O (1989) Functional characterization of a rat dopamine D-2 receptor cDNA expressed in a mammalian cell line. Mol Pharmacol 36:446–451.

Palm D, Munch G, Dees C, Hekman M (1989) Mapping of β-adrenoceptor coupling domains to G_s-protein by site-specific synthetic peptides. FEBS Lett 254:89–93.

Potenza MN, Lerner MR (1991) A recombinant vaccinia virus infects *Xenopus* melanophores. Pigment Cell Res 4:186–192.

Potenza MN, Lerner MR (1992) A rapid quantitative bioassay for evaluating the effects of ligands upon receptors that modulate cAMP levels in a melanophore cell line. Pigment Cell Res 5:372–378.

Potenza MN, Graminski GF, Lerner MR (1992) A method for evaluating the effects of ligands upon G_s protein coupled receptors using a recombinant melanophore-based bioassay. Anal Biochem 206:315–322.

Potter H (1988) Electroporation in biology: methods, applications and instrumentation. Anal Biochem 174:361–373.

Potter H, Weir L, Leder P (1984) Enhancer-dependent expression of human κ immunoglobulin genes introduced into mouse Pre-B lymphocytes by electroporation. Proc Natl Acad Sci USA 81:7161–7165.

Richelson E (1988) Neuroleptic binding to human brain receptors: relation to clinical effects. Ann NY Acad Sci 537:435–442.

Robbins TW (1990) The case for frontostriatal dysfunction in schizophrenia. Schizophr Bull 16:391–401.

Ruffolo RR Jr, Shaar CJ (1983) Relative potency of LY141865 at dopamine DA_2 and histamine H_2 receptors. Eur J Pharmacol 92:295–296.

Seeman P (1992) Dopamine receptor sequences—therapeutic levels of neuroleptics occupy D2-receptors, clozapine occupies D4. Neuropsychopharmacol 7:261–284.

Seeman P, Grigoriadis D (1987) Dopamine receptors in brain and periphery. Neurochem Int 10:1–25.

Seeman P, Niznik H (1988) Dopamine D_1 receptor pharmacology. ISI Atlas Sci 2:161–170.

Sibley DR, Monsma FJ Jr (1992) Molecular biology of dopamine receptors. Trends Pharmacol Sci 13:61–69.

Sibley D, Leff S, Creese I (1982) Interactions of novel dopaminergic ligands with D-1 and D-2 dopamine receptors. Life Sciences 31:637–645.

Snyder LA, Roberts JL, Sealfon SC (1991) Alternative transcripts of the rat and human dopamine D_3 receptor. Biochem Biophys Res Commun 180:1031–1035.

Snyder SH (1973) Amphetamine psychosis: a "model" schizophrenia mediated by catecholamines. Am J Psychiatry 130:61–67.

Sokoloff P, Giros B, Martres M-P, Bouthenet M-L, Schwartz J-C (1990) Molecular cloning and characterization of a novel dopamine receptor (D_3) as a target neuroleptics. Nature 347:146–151.

Sokoloff P, Andrieux M, Besancon R, Pilon C, Martres M-P, Giros B, Schwartz J-C (1992) Pharmacology of human dopamine D3 receptor expressed in a mammalian cell line: comparison with D2 receptor. Eur J Pharmacol 225:331–337.

Stevens JR (1973) An anatomy of schizophrenia. Arch Gen Psychiatry 29:177–189.

Stoof JC, Kebabian JW (1984) Two dopamine receptors: biochemistry, physiology, and pharmacology. Life Sci 35:2281–2296.

Stormann TM, Gdula DC, Weiner DM, Brann MR (1990) Molecular cloning and expression of a dopamine D2 receptor from human retina. Mol Pharmacol 37:1–6.

Sugden D (1991) Aggregation of pigment granules in single cultured *Xenopus laevis* melanophores by melatonin analogues. Br J Pharmacol 104:922–927.

Sunahara RK, Niznik HB, Weiner DM, Stormann TM, Brann MR, Kennedy JL, Gelernter JE, Rozmahel R, Yang Y, Israel Y, Seeman P, O'Dowd BF (1990) Human dopamine D_1 receptor encoded by an intronless gene on chromosome 5. Nature 347:80–83.

Sunahara RK, Guan H-C, O'Dowd BF, Seeman P, Laurier LG, Ng G, George SR, Torchia J, Van Tol HHM, Niznik HB (1991) Cloning of the gene for a human dopamine D_5 receptor with higher affinity for dopamine than D_1. Nature 350:614–619.

Tang L, Hickok J, Harmon S, Todd RD, O'Malley KL (1992) Characterization of D2, D3, and D4 dopamine receptors expressed in the same cell background. Soc Neurosci Abstr 18:7.

Tiberi M, Jarvie KR, Silvia C, Farlardeau P, Gingrich JA, Godinot N, Bertrand L, Yang-Feng TL, Fremeau RT Jr, Caron MG (1991) Cloning, molecular characterization, and chromosomal assignment of a gene encoding a second D1 dopamine receptor subtype: differential expression pattern in rat brain compared with the D1A receptor. Proc Natl Acad Sci USA 88:7491–7495.

Van Tol HHM, Bunzow JR, Guan H-C, Sunahara RK, Seeman P, Niznik HB, Civelli O (1991) Cloning of the gene for a human dopamine D_4 receptor with high affinity for the antipsychotic clozapine. Nature 350:610–614.

Van Tol HHM, Wu CM, Guan H-C, Ohara K, Bunzow JR, Civelli O, Kennedy J, Seeman P, Niznik HB, Jovanovic V (1992) Multiple dopamine D_4 receptor variants in the human population. Nature 358: 149–152.

West RE Jr, Moss J, Vaughan M, Liu T, Liu T-Y (1985) Pertussis toxin–catalyzed ADP-ribosylation of transducin. Cysteine 347 is the ADP-ribose acceptor site. J Biol Chem 260:14428–14430.

Zhou Q-Y, Grandy DK, Thambi L, Kushner JA, Van Tol HHM, Cone R, Pribnow D, Salon J, Bunzow JR, Civelli O (1990) Cloning and expression of human and rat D_1 dopamine receptors. Nature 347:76–80.